

A REFLECTARRAY ANTENNA BACKED ON FSS FOR LOW RCS AND HIGH RADIATION PERFORMANCES

H. Li, B.-Z. Wang, G. Zheng, and W. Shao

Institute of Applied Physics
University of Electronic Science and Technology of China
Chengdu 610054, China

L. Guo

Department of Physics
Xinjiang Kashi Teacher's College
Kashi 844000, China

Abstract—This paper investigates the application of frequency-selective surface (FSS) in reflectarray antennas for the purpose of reducing radar cross section (RCS) level. Different from previous reports, the presented band-stop FSS structure is also characterized by the suppression of surface waves, which makes a contribution to better radiation performance. Two 14×14 reflectarray antennas backed on the FSS ground and a solid ground are designed and fabricated. Simulated and measured results show that the FSS ground can improve the ‘in-band’ gain by 1.1 dB, decrease the sidelobe level by 6.4 dB, and reduce the ‘out-of-band’ RCS effectively when compared with the antenna with a solid ground plane of the same size.

1. INTRODUCTION

A reflectarray antenna is a low profile reflector consisting of a planar array of microstrip patches, with a certain tuning to produce prescribed beam shape and direction when illuminated by a primary source [1–5]. Due to its properties of being flat, light weight, low cost, and high gain, reflectarray antenna is rapidly becoming an attractive alternative to the traditional parabolic reflector antenna in the applications where high gain antenna is needed [6]. However, it is well known that

the use of high-gain antennas on military platforms (aircraft, ships, and so on) increases radar cross section (RCS) levels and platform detectability, even though the antennas are very well matched to their feeding circuit [7].

There are common ways for RCS reduction, including coating with radar-absorbing materials [8], antenna shaping [9,10], using passive and active cancellation technology [11–12], and employing frequency-selective surfaces (FSS) [13] as the reflector. Considering the spatial excitation structure of reflectarray antenna, coating with radar-absorbing materials is obviously not a good option for its bulky configuration. Moreover, antenna shaping or passive/active loads to every element will increase complexity and cost. And therefore, the last solution with the use of an FSS ground plane is considered in this study. Reference [13] provided an FSS-backed reflectarray and demonstrated that the ‘out-of-band’ reflectivity of the antenna is reduced by more than 4 dB when the solid conducting ground plane is replaced with a bandstop frequency-selective surface. However, there is no discussion about the preservation/deterioration of the antenna radiation performances in [13]. In fact, high gain and low sidelobe (SLL) are very important for long distance radar communications where reflectarray antenna is employed. Therefore, the RCS reduction of reflectarray antenna without sacrificing its radiation characteristics, or even improving some of the radiation performances is the aim of this paper.

Enhancement of antenna gain may be achieved by using electromagnetic bandgap (EBG) structures. EBG structures, also called photonic bandgap (PBG) structures [14–16], offer pass- and stop-bands to electromagnetic waves in the same way semiconductors offer these properties to electrons. When the operation frequencies fall into the surface-wave bandgap, it is possible to forbid the surface-wave propagation in a plane and therefore achieve a high gain radiation pattern. This technique was verified in reflectarray antenna by Shum et al. [17] incorporating an EBG structure consisting of a periodic array of perforations in the ground plane. With this approach, the gain is increased by 2.5 dB. However, no RCS reduction results are reported with such EBG ground plane in [17].

FSS and EBG are both planar periodic structures having filtering-wave function, the former for spatial waves, and the latter for surface waves. So it is possible to design an FSS structure, also characterized by the suppression of surface waves, if only both the stop-bands can cover the operation frequency band of the reflectarray.

In this paper, two 14×14 reflectarray antennas backed on the FSS and a solid ground are designed and fabricated. Simulated and

measured results show that the FSS ground can improve the ‘in-band’ gain by 1.1 dB, decrease the sidelobe level by 6.4 dB, and reduce the ‘out-of-band’ RCS effectively, compared with the antenna with a solid ground plane of the same size. Although the introduction of FSS into reflectarray antennas has been reported, the application of FSS structure to reflectarray for low RCS, low sidelobe, and high gain synchronously, to the authors’ knowledge, does not exist as yet.

2. DESIGN PROCEDURE

2.1. Design of Reflectarray Antenna Element

In order to expand the reflectarray antenna bandwidth, a single-layer and dual resonant windmill-shaped element structure is designed as shown in Fig. 1 [18]. Because the phase characteristic acquired for the normal wave incidence provides a good approximation for the cases of TE and TM wave incidence for an angle up to 30° from the reflectarray boresight direction [19], normal wave incidence is considered to obtain phase characteristic. The interaction of a normal incidence plane wave with the reflectarray can be modeled numerically by a unit cell waveguide approach (WGA) [19,20]. As displayed in Fig. 2, a reflectarray element is placed in a waveguide with a square cross section. Since the top and bottom walls of the waveguide are perfect magnetic conductors (PMC) and its side walls are perfect electric conductors (PEC), the waveguide can support a TEM plane wave, and in the following, we take a simulation of the structure with the

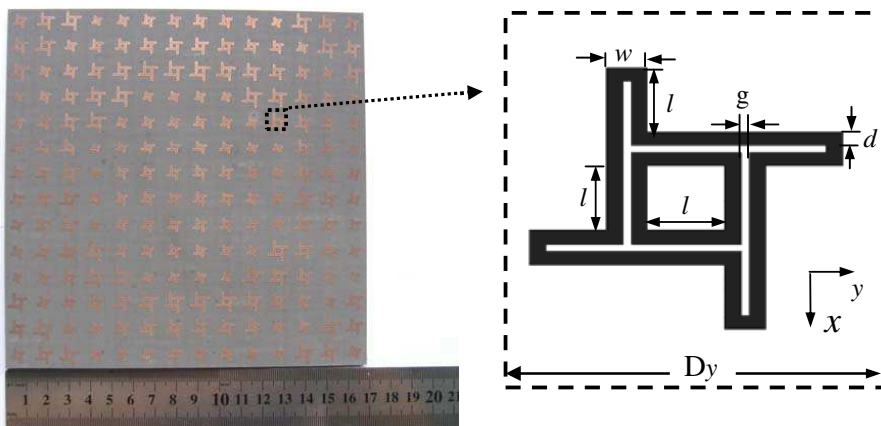


Figure 1. Top view of a reflectarray antenna.

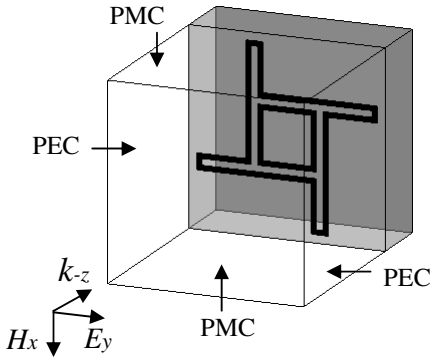


Figure 2. Sketch map of WGA.

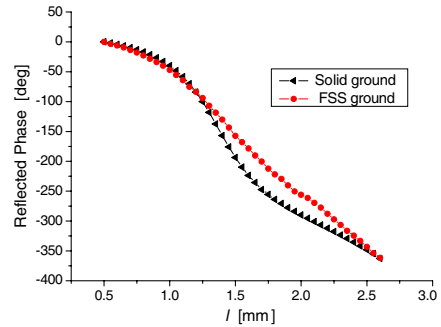


Figure 3. Photograph of the practical FSS ground.

commercial electromagnetic software Ansoft HFSS. In the simulation, a y -polarized plane wave propagating in $-z$ direction is cast upon the structure with $w = 1$ mm, $g = 0.4$ mm, $\varepsilon_r = 2.65$, $t = 4$ mm, and $l = 0.5$ mm \sim 2.6 mm, and then the reflected-phase response is computed. Based on the results presented in Fig. 3, by simple adjustment of the elements size, we obtain a phase variation in the range of around 360° and quasi-linear reflection phase variation with element size, which could help to expand the bandwidth.

2.2. FSS Design

To reduce the ‘out-of-band’ RCS of the proposed reflectarray antenna, the solid ground is replaced with a band-stop frequency-selective surface named gridded square [21]. The practical configuration of the FSS ground is shown in Fig. 4. It is composed of a periodic array of perforations in the ground plane. An element consists of two perforations: a square loop outside and a square inside. The elements are periodic in two dimensions (x and y) with equal periods of $D_x = D_y = 0.5\lambda_0$. E_L is the side length of square perforation, E_d is the separation between the two perforations, and E_g is the width of the square loop.

In view of the reflectarray elements on the top of the substrate exert an influence on the frequency-selective characteristic of the FSS ground, the reflectarray element will be considered in the computation of spatial-wave stopband. The transmission coefficient S_{12} analysis is also carried out by WGA.

It is generally known that an electrically thick microstrip substrate can sustain a considerable amount of surface wave energy. As a

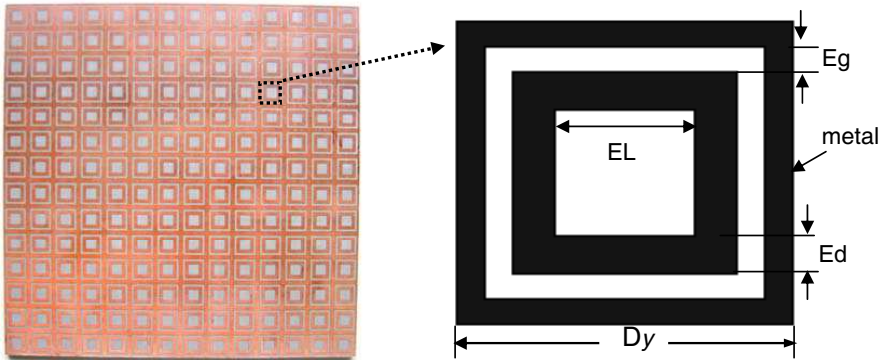


Figure 4. Photograph of the practical FSS ground.

result, it will generate significant substrate surface coupling, which is especially strong for a substrate thickness of greater than $0.1\lambda_0$ (λ_0 is the free space wavelength [22]). In our design, the ‘Suspending Micro-strip Method’ proposed in [23] is used to investigate the surface-wave stopband of the proposed FSS structure, as shown in Fig. 5. Same as the computation of the spatial-wave stopband, the reflectarray elements are also involved in the evaluation of surface-wave stopband. A two-dielectric-layer structure is placed in a waveguide. The underlayer is a substrate ($\epsilon_r = 2.65$) with 7 reflectarray elements on the top side and 7 FSS elements at the bottom. The superstratum is a low-dielectric constant ($\epsilon_r = 1.03$) foam layer with a thickness of $t/2$ (t is the thickness of the substrate), which is used to support the $50\ \Omega$ -microstrip line. Surface waves are launched along the underlayer substrate by a waveport, and are detected by another waveport aligned with the first one. And hence, propagation characteristic of surface wave can be obtained by transmission coefficient S'_{12} (superscript is used to distinguish two transmission coefficients in this paper). Only one row of elements are necessary because the fields in the microstrip line are concentrated near the line.

The operation frequency band of the reflectarray antenna in this paper is from 11.7 GHz to 13.9 GHz, so the spatial-wave stopband and the surface-wave stopband of the proposed FSS should both cover this frequency band. After an optimization procedure, the structural parameters are designed as: $E_L = 5\ \text{mm}$, $E_d = 1.5\ \text{mm}$, and $E_g = 1\ \text{mm}$.

Figure 6 shows the spatial-wave transmission coefficients of the FSS element combined with the reflectarray elements of different sizes, for $l = 0.5\ \text{mm}$, $l = 1.3\ \text{mm}$, and $l = 2.6\ \text{mm}$ respectively. As can be

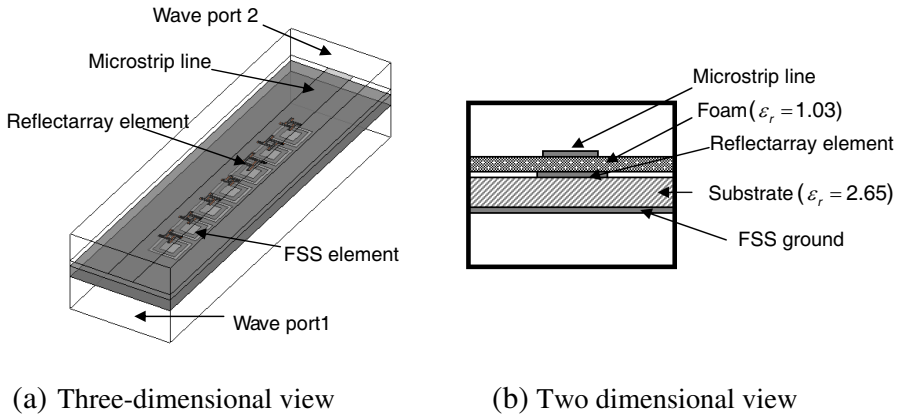


Figure 5. Sketch map of the ‘Suspending Micro-strip Method’.

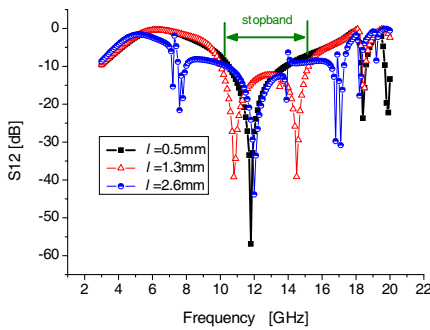


Figure 6. Simulated spatial-wave transmission coefficients of the designed FSS element.

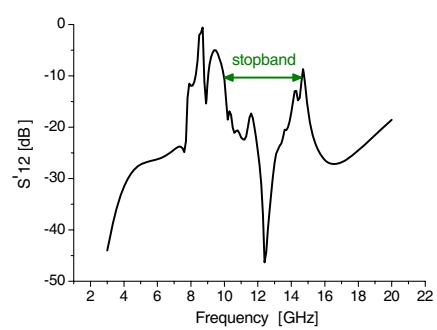


Figure 7. Simulated surface-wave transmission coefficient of designed FSS structure.

observed from Fig. 6, the transmission coefficient drops below 10 dB from 10.5 GHz to 13.8 GHz for $l = 0.5$ mm, from 10.1 GHz to 15.1 GHz for $l = 1.3$ mm, and from 10.4 GHz to 13.6 GHz for $l = 2.6$ mm. From a holistic angle of view, this means that spatial electromagnetic wave is reflected in a rough region covering 10.3 GHz \sim 14.5 GHz, corresponding to the reflecting band about 4.2 GHz wide. Although the spatial-wave stopband of the designed FSS element is wider than the operation band, the actual spatial-wave stopband is close to the region of 11.7–13.9 GHz, due to the practical array environments, which will be demonstrated by RCS in Section 3.

The surface-wave transmission coefficient of the designed FSS structure is displayed in Fig. 7. As can be observed, the surface-

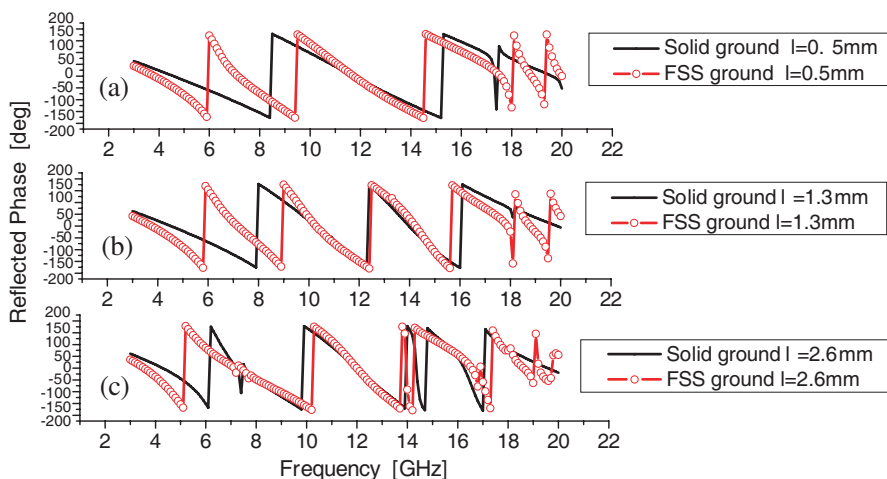


Figure 8. Reflected phase against frequency of two reflectarray elements backed on solid ground and FSS ground. (a) $l = 0.5$ mm, (b) $l = 1.3$ mm, (c) $l = 2.6$ mm.

wave bandgap is set from 10.1 GHz to 15.05 GHz so as to ensure the enhancement of reflected electromagnetic energy in the antenna's operation frequency band.

As the FSS replaces the solid ground, the reflected phase curve must be recalculated. As displayed in Fig. 3, a low Q linear phase response is preserved when the solid ground is replaced with the FSS ground. Moreover, the phase responses with frequency variation for reflectarray element with solid ground and FSS ground are also compared in Fig. 8, for $l = 0.5$ mm, $l = 1.3$ mm, and $l = 2.6$ mm respectively. The 'in-band' (11.7 GHz–13.9 GHz) reflection phase responses of the two structures are similar.

3. RESULTS

In order to examine the validation of replacing the solid ground with the proposed FSS structure, two 14×14 reflectarrays are carefully designed and fabricated. The reflectarrays are centre fed by a linearly-polarized horn located 11.2 cm away to maximize the illumination efficiency. Considering the configuration of a standard microstrip reflectarray in Fig. 9, the progressive phase distribution on the reflectarray surface that produces a beam in the direction $\hat{r}_0(\theta_b, \phi_b)$,

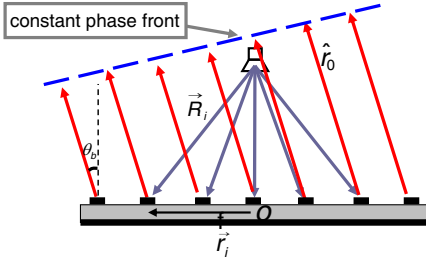


Figure 9. Configuration of microstrip reflectarray.

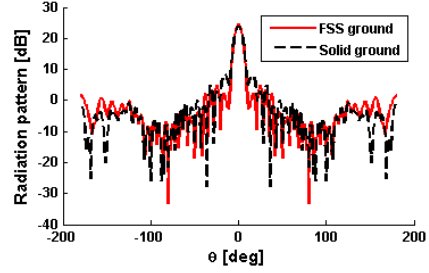


Figure 10. Measured radiation patterns of two antennas.

as known from array theory, is expressed as [1]

$$\phi_i = 2\pi N + k_0(R_i - \vec{r}_i \cdot \hat{r}_0) \quad (N = 0, 1, 2 \dots) \quad (1)$$

where k_0 is the propagation constant in vacuum, \vec{R}_i is the position vector from the phase center of feed horn to the i th element, \vec{r}_i is the position vector from the array center to the i th element. In this design, $\varphi_b = 90^\circ$, $\theta_b = 0^\circ$. The sizes of all the elements are determined by using (1) and the phase curves shown in Fig. 3. The radiation patterns are measured in a SATIMO chamber at 12.5 GHz which is in the stopband of the FSS structure. Fig. 10 shows the comparison of the measured radiation patterns of two antennas. The dash line indicates the radiation pattern of the reflectarray with solid ground, and the solid line is that of the reflectarray with FSS ground. Due to the slot design of antenna ground, some energy radiates in the backward direction. Therefore, the back lobe of the reflectarray with FSS ground increases by about 2.1 dB compared to the original antenna. However, the 3 dB beamwidth of the reflectarray with FSS ground decreases from 8.2° to 7.9° , and the sidelobe level also decreases by about 6.4 dB. And consequently, the antenna gain increases about 1.1 dB. In addition, Fig. 11 depicts the measured gain bandwidth of the two reflectarrays. It can be observed that the 1-dB gain bandwidth of the reflectarray backed on FSS is 1.5 GHz (12–13.5 GHz), which has a moderate discrepancy compared to the original antenna (2.2 GHz, 11.7–13.9 GHz). Overall, the measured results show the radiation characteristics in upper half-space of the reflectarray backed on FSS are preserved.

In this section, the relationship between monostatic RCS at incident angle ($\varphi = 90^\circ$, $\theta = 0^\circ$) and the frequencies of two antennas is presented to validate the proposed method. When the incident frequency exceeds the operation band of the antenna, most of the

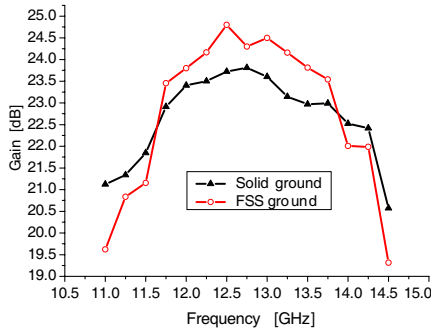


Figure 11. Measured gain versus frequency.

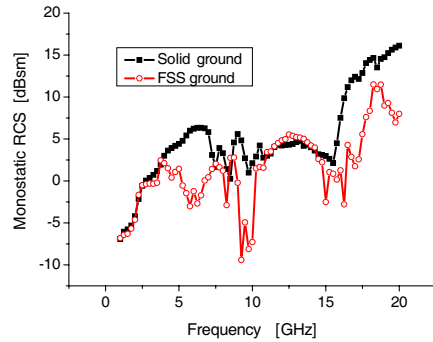


Figure 12. Simulated monostatic RCS versus frequency.

electromagnetic energy will be reflected back to the upper half-space for the solid ground case. Whereas due to the band-pass characteristic of the FSS ground, the incident wave will propagate through the antenna. As a result, the ‘out-of-band’ RCS will be reduced dramatically. Fig. 12 shows the monostatic RCS for the vertical incidence case in the frequency range of 2–18 GHz. It can be seen that there is evident RCS reduction out of band, especially a maximum RCS reduction of 15 dBsm occurs at 9.1 GHz. For the ‘in-band’ frequencies, the FSS works as a solid ground, and together with the surface-wave suppression, the RCS level increases slightly.

4. CONCLUSION

The integration of FSS into reflectarray antenna for RCS reduction and preservation of radiation performances has been shown and validated with simulation and measurements. The results show that the FSS ground can improve the ‘in-band’ gain by 1.1 dB, decrease the sidelobe level by 6.4 dB, and reduce the ‘out-of-band’ RCS effectively when compared with the antenna with solid ground plane of the same size.

ACKNOWLEDGMENT

This work was supported by the National Natural Science Foundation of China (No. 60901023), the High-Tech Research and Development Program of China (No. 2008AA01Z206), and Project 9140A01020110DZ0211.

REFERENCES

1. Pozar, D. M., S. D. Targonski, and H. D. Syrigos. "Design of millimeter wave microstrip reflectarrays," *IEEE Trans. Antennas Propagat.*, Vol. 45, 287–296, Feb. 1997.
2. Sayidmarie, K. H. and M. E. Bialkowski, "Phasing of a microstrip reflectarray using multi-dimensional scaling of its elements," *Progress In Electromagnetics Research B*, Vol. 2, 125–136, 2008.
3. Venneri, F., S. Costanzo, and G. Di Massa, "Transmission line analysis of aperture-coupled reflectarrays," *Progress In Electromagnetics Research C*, Vol. 4, 1–12, 2008.
4. Venneri, F., S. Costanzo, G. Di Massa, and G. Amendola, "Aperture-coupled reflectarrays with enhanced bandwidth features," *Journal of Electromagnetic Waves and Applications*, Vol. 22, No. 11–12, 1527–1537, 2008.
5. Tahir, F. A., H. Aubert, and E. Girard, "Equivalent electrical circuit for designing MEMS-controlled reflectarray phase shifters," *Progress In Electromagnetics Research*, Vol. 100, 1–12, 2010.
6. Huang, J. and J. A. Encinar, *Reflectarray Antennas*, John Wiley & Sons Inc., Hoboken, NJ, 2007.
7. Collardey, S., A.-C. Tarot, P. Pouliguen, and K. Mahdjoubi, "Use of electromagnetic band-gap materials for RCS reduction," *Microwave and Optical Technology Letters*, Vol. 44, 546–550, Mar. 2005.
8. Bhattacharyya, A. K., "Radar cross section reduction of a flat plate by RAM coating," *Microwave and Optical Technology Letters*, Vol. 3, 324–327, Sep. 1990.
9. Li, Y., Y. Liu, and S.-X. Gong, "Microstrip antenna using ground-cut slots and miniaturization techniques with low RCS," *Progress In Electromagnetics Research Letters*, Vol. 1, 211–220, 2008.
10. Zheng, J.-H., Y. Liu, and S.-X. Gong, "Aperture coupled microstrip antenna with low RCS," *Progress In Electromagnetics Research Letters*, Vol. 3, 61–68, 2008.
11. Chambers, B. and A. Tennant, "General analysis of the phase-switched screen, Part 1: The single layer case," *Radar Sonar and Navigation*, Vol. 149, No. 5, 243–247, Oct. 2002.
12. Zheng, Q.-R., Y.-M. Yan, X.-Y. Cao, and N.-C. Yuan, "High impedance ground plane (HIGP) incorporated with resistance for radar cross section (RCS) reduction of antenna," *Progress In Electromagnetics Research*, Vol. 84, 307–319, 2008.
13. Misran, N., R. Cahill, and V. F. Fusco, "RCS reduction technique

- for reflectarray antennas,” *Electron. Lett.*, Vol. 39, 1630–1631, Nov. 2003.
14. Moghadasi, S. M., A. R. Attari, and M. M. Mirsalehi, “Compact and wideband 1-D mushroom-like EBG filters,” *Progress In Electromagnetics Research*, Vol. 83, 323–333, 2008.
 15. Shaban, H. F., H. A. Elmikatay, and A. A. Shaalan, “Study the effects of electromagnetic band-gap (EBG) substrate on two patches microstrip antenna,” *Progress In Electromagnetic Research B*, Vol. 10, 55–74, 2008.
 16. Zhang, L.-J., C.-H. Liang, L. Liang, and L. Chen, “A novel design approach for dual band electromagnetic band gap structure,” *Progress In Electromagnetic Research M*, Vol. 4, 81–91, 2008.
 17. Shum, K. M., Q. Xue, C. H. Chan, and K. M. Luk, “Gain enhancement of microstrip reflectarray incorporating a PBG structure,” *Microwave and Optical Technology Letters*, Vol. 28, 114–116, Jan. 2001.
 18. Li, H., B.-Z. Wang, and P. Du, “Novel broadband reflectarray antenna with windmill-shaped elements for millimeter-wave application,” *Intl. Journal of Infrared & Millimetre Waves*, Vol. 28, 339–344, Mar. 2007.
 19. Tsai, F.-C. E. and M. E. Bialkowski, “Designing a 161-element Ku-band microstrip reflectarray of variable size patches using an equivalent unit cell waveguide approach,” *IEEE Trans. Antennas Propag.*, Vol. 51, 2953–2962, Oct. 2003.
 20. Bialkowski, M. E. and K. H. Sayidmarie, “Bandwidth considerations for a microstrip reflectarray,” *Progress In Electromagnetics Research B*, Vol. 3, 173–187, 2008.
 21. Lee, C. K., R. J. Langley, and E. A. Parker, “Single layer multiband frequency selective surfaces,” *IEE Proceedings Part H*, Vol. 132, 411–412, 1985.
 22. Bamford, L. D., J. R. James, and A. F. Fray, “Minimising mutual coupling in thick substrate microstrip antenna arrays,” *Electronics Lett.*, Vol. 33, 648–650, Apr. 1997.
 23. Radisic, V., Y. Qian, and R. Coccioli, “Novel 2-D photonic bandgap structure for microstrip lines,” *IEEE Microwave Guided Wave Lett.*, Vol. 8, 69–71, Feb. 1998.